Optimal Synthesis of Integrated Reactive Distillation Systems for Fischer-Tropsch Process

Naien He

Report for the degree of Master of Science

Table of Contents

ABSTRACT **3**

INTRODUCTION **4**

1 PROBLEM STATEMENT **5**

1.1 PRODUCT QUALITY 5
1.2 OPERATION SCALE 5
1.3 COLUMN CONFIGURATION 6
1.4 ECONOMIC OBJECTIVE 7

2 METHODS **8**

2.1 MODEL FORMULATION 8
2.2 INITIALIZATION 9
2.3 MULTI-START 10
2.4 OPTIMIZATION 11

3 RESULTS AND DISCUSSION **13**

3.1 SUCCESS RATE 13
3.2 OPTIMIZATION STATISTICS 17
3.3 PROFIT 23
3.4 OPTIMUM RESULTS 26
3.5 COMPARISON WITH REACTIVE FLASH 32

4 CONCLUSION **36**

5 BIBLIOGRAPHY **38**

Abstract

Fischer-Tropsch (FT) is an important reaction that bridges the gap between inorganic syngas and transportation fuels such as gasoline. It is receiving more and more attention today as a technology to produce transportation fuels from coal, also from stranded natural gas produced from remote oil field.

Reactive distillation (RD) is a proven reactive separation method that can save downstream separating cost by performing separating and reaction simultaneously. In addition to that, it can enhance yield by constantly removing by-products and thus create favorable zones for reaction equilibrium. It can also enhance conversion by increasing reactant concentration by means such as enhanced gas phase feed solubility in liquid phase.

In this work, we built a rigorous mathematical model to simulate and optimize a FT reactive distillation column (Y. Hu Masters report), with an economic objective that favors the production of gasoline. Solution strategy including initialization and globalization will be implemented and tested. The result indicated that reactive distillation can offer a much better performance than baseline slurry phase reactive flash, in terms of both conversion and selectivity.

Introduction

Currently a large portion of the world's fuel production is based on petroleum crude oil. As the crude reserve is depleting at fast pace, a lot of interests has shifted to finding alternative ways to sustain ever-growing fuel consumption. With the fast development of processes to convert coal or methane to synthesis gas, Fischer-Tropsch (FT) process has received a lot of attention as it can convert synthesis gas directly to liquid fuel.

At the present time, a few design criteria are critical to the commercial success of a FT process. The first is the how to maximize the yield of high-value product. Second is how to reduce capital requirement by reducing the number of downstream operations. Third is how to make use of the large amount of heat released by the reaction and feed them into energy consuming separating process. Historically improvements on FT reactor design have been primarily focused on heat removal and reducing catalyst loading, as a result, little attention has been given to reduce the large CAPEX and OPEX involved in the downstream separating process of FT reaction.

Reactive distillation (RD) is a proven reactive separation method that can reduce capital investment by combining reaction and separation equipment into one. It can also be used to save downstream separating cost by using the heat generated from reaction as heat source. In addition to that, it can enhance yield by constantly removing by-products and thus create favorable zones for reaction equilibrium. It can also enhance conversion by increasing reactant concentration by means such as enhanced gas phase feed solubility in liquid phase.

In previous works (Srinivas, Malik, Mahajani, 2008), an Aspen model consists of 6 stages are simulated. The author modified RadFrac module with a simplified kinetics equation. Without any optimization, the authors showed an improvement over traditional slurry phase reactive flash reactor. In recent works (Zhang, Masuku, Biegler, 2018) a equation-oriented model for 7-stage FT reactive distillations have been developed and successfully solved in GAMS. The model contains rigorous kinetics, VLE and energy model, which are referenced in this work as base formulation. By optimizing that model, the authors were able to show substantial improvement over slurry phase reactor.

In this work, we will first build upon the base model with a 20-tray formulation. We will expand the model's capability to seamlessly model phase transitions with MPCC formulation. We will also expand the optimization problem from operation variables to design variables such

as catalyst and feed allocation, product and reflux tray selection. To solve the model at a much larger scale, we will construct an algorithm that could reliably solve the same reactive distillation model up to 50 stage count. We will then investigate different methods to globalize the solution and discuss features of the optimum solution. Lastly, we will conduct sensitivity analysis on the optimum solution and discuss how key parameters could affect optimal design.

1 Problem Statement

From a design perceptive, the design criteria given to a FT reactive distillation column aims at produce gasoline is as follows:

1.1 Product Quality

FT reaction produces a very wide range of products with operating pressure at 20 bar, which is difficult to directly distillate to commercial grade products. Nevertheless, a strong separation could still be made. In this report we will define product separation rules as follows:

Product Type	Component of Interest	Percentage
Naphtha	C5 – C7	> 75 %
Heavy Naphtha	N/A	N/A
Gasoline	C8 – C12	> 75 %
Diesel	C13 – C18	> 75 %
Heavy	C19 – C56	> 75 %

In later portions of this report, an analysis of product produced using this specification is conducted using specifications used in commercial product, such as density and distillation curve, to verify that the product specification is able to further refine to commercial grade.

1.2 Operation Scale

To establish a baseline for comparison, a fixed amount of consumption is set:

Material	Amount	Specification
Feed	10 kmol/s	H2:CO = 2:1
Catalyst	30000 kg	Operating Temperature 200°C - 300°C

Note that only one of the two variables listed above is needed to define the scale of the distillation column. As a result, one of the variables could be factored into the overall cost function and be optimized. Here, we will choose to fix the total amount of catalyst and relax total feed. Nevertheless, the values provided above could be used for initialization into a baseline design.

1.3 Column Configuration

	Features	Value
Fixed	Total tray number	20
	Non-reactive (adiabatic)	1-7
	Pressure (bar)	20
	Condenser Pressure (bar)	19
	Condenser Temperature	30
	Reboiler Pressure (bar)	20
	Reboiler Temperature	350
	Feed Temperature	200
Variable	Distillate ratio	[0.05,1]
	Heavy naphtha location	[1,2]
	Gasoline location	[3,9]
	Diesel location	[10,18]
	Temperature (Adiabatic)	[100,350]
	Temperature (Reactive)	[200,300]
	Catalyst	[100,30000]
	Feed	[0.01,10]

Principally, apart from observing physical constraints of the catalyst, the column configuration should be completely open to optimization. Nevertheless, some addition constraints are added and explained below in detail:

1. Total tray number is given as an upper bound for the system, as tray number will be reduced during optimization given economic objective.
2. As discussed in the reactive flash case study, non-reactive (adiabatic and remove temperature constraints) stages are necessary to account for the low boiling point of reflux flow. The selection right now is arbitrary and based on experience. Unfortunately, the selection also has to be done beforehand, due to the fact that adiabatic model is different from reactive model.
3. Column operating pressure is fixed based on catalyst operating condition. Feed temperature is also fixed as it is easily interchangeable with tray duty, and they combined heat duty remains the same.
4. Distillate ratio and product tray location constraints are set based on experience. Lower bound on catalyst and feed is imposed to avoid numerical difficulty.

1.4 Economic Objective

Having a realistic economic objective is critical to the accuracy of the model and the optimum solution. Therefore, a list of economic objectives is compiled from various sources, to establish a realistic weight to each product.

1.4.1 C1, C2 and LPG

Typically, there are multiple processes for light hydrocarbons separation, from simple liquefying process to produce LNG and LPG, to complicated distillation process to extract olefins. The exact process is beyond the scope of this case study, furthermore, the majority of this product consists of methane and unreacted syngas, which could be recycled back to the process. Therefore, we estimate the economic value for this portion to be 60% of the syngas full cost.

1.4.2 Naphtha

Naphtha currently trades international at around $650/ton. Assuming an average molecular weight of 84g/mol, the current price for naphtha is $54/kmol. Factoring in cost of further refining and blending. The estimated value for naphtha product is at $43/kmol.

1.4.3 Heavy Naphtha

In this process the presence of heavy naphtha is primarily used to trim light tail of gasoline product, as a result its quality is not constrained. Therefore, heavy naphtha is a by-product of this process. We estimate the value for heavy naphtha product at $20/kmol.

1.4.4 Gasoline

Current prices (https://www.eia.gov/todayinenergy/prices.php) for wholesale gasoline is at $2.3 per gallon. Assuming 6.3 pounds per gallon, 0.45 kg per pound, and an average molecular weight of 140 g/mol, the current price for gasoline is $112/kmol. Factoring in cost of further refining and blending. The estimated value for gasoline product is at $90/kmol.

1.4.5 Diesel

Current prices (https://www.eia.gov/todayinenergy/prices.php) for wholesale diesel is at $2.4 per gallon. Assuming 6.9 pounds per gallon, 0.45 kg per pound, and an average molecular weight of 210 g/mol, the current price for diesel is $161/kmol. Factoring in cost of further refining and blending. The estimated value for diesel product is at $128/kmol.

1.4.6 Heavy

Fully refined wax currently trades for $1000/ton. Assuming an average molecular weight of 350 g/mol, the current price for heavy is $350/kmol. Factoring in large amount of quality deficiency. The estimated value for heavy product is at $100/kmol.

1.4.7 Tray / Reactive Stage

The total cost of the distillation column is hard to estimate, and not necessary for the purpose of this case study. The cost saving provided by each tray, however, could provide useful insights into the economic size of the reactive distillation column. We estimate the capital cost and total maintenance cost for the entire reactive distillation column is around $30M. Assuming a 10-year depreciating period, the cost of each tray is $0.005/s.

1.4.8 Feed Gas

Assuming syngas is generated from either coal gasification or methane reforming, based on past working experience with both technologies, we estimate the full cost for syngas is around $0.1 per standard cubic meter, which is $2.24/kmol.

1.4.9 Heat Duty

FT reaction is extremely exothermic, as a result, the majority of heat duty is in the form of cooling with the potential of generating process steam. Therefore, in this case study heat duty cost will be ignored.

2 Methods

2.1 Model Formulation

The model consists of 3 parts, more details can be found in Y. Hu's masters report, or on the GitHub page: https://github.com/naienh/FT-Reactive-Distillation-Pyomo.

Part	Equation Block
Basic	Kinetics
	VLE
	VLLE
	Enthalpy
	MESH
Phase Transition	MPCC
Discrete Variable	DDF

2.2 Initialization

An average FT reactive distillation model with 20 trays have 30k variables and equations, most of them are highly non-linear. Therefore, a successful initialization is required before the model could be further optimized. To initialize the model, a set of variables must be specified to define the model. Here, we will discuss which variables are selected and how their values are set before optimization starts.

One of the most common way to initialize the model is to simply solve for a feasible solution that satisfies all the constraints, specifically the quality constraint. However, in this case study, a few difficulties arose when applying this technique:

1. Quality constraints are complicated inequalities involving multiple components. Because of this, the correlation between quality and all other design elements is not straightforward. As a result, it is not guaranteed that a model could even have a feasible solution when factoring in other design elements.
2. Initialization based on quality constraint is much harder to succeed when compared to sequential method we discussed in previous works. Since all related design elements must be relaxed to search for a feasible solution, the problem becomes another optimization problem, which is hard to solve without, again, proper initialization.
3. Because all related design elements are required to be relaxed, even if the initialization succeeds, the solution is often funneled into a very specific region where quality constraints are the easiest to meet. This means that the user has very limited control over values of other variables after initialization. This could be difficult for globalization strategies such as multi-start to ensure a uniform distribution.

To summarize, initialization directly to a feasible solution for reactive distillation is difficult as it requires the relaxation of all variables similar to an optimization problem. Even it is successful, it limits the distribution of potential starting points to solutions that are the easiest to meet quality constraints. To ensure high success initialization rate and a wide distribution of start points, an operability-based initialization method is chosen for this case study.

The operability region, as its name suggests, is a collection of all the manipulatable variables during column operation, such as temperature / duty, reflux and flow rates. These variables have the following characteristics:

1. They are independently adjustable, and a solution is guaranteed to converge, provided they are within bounds. This ensures that the initialization can be done sequentially by adjusting their values one by one.
2. Fixing these variables fully defines the system. This means that the system is initialized with no degrees of freedom, which improves success rate and gives user full control of the state the system is in after initialization.

2.3 Multi-start

Multi-start is very effective to search for global minima by allowing the system to start in different regions. Traditional multi-start algorithm typically randomizes all variables within their respective bounds, then optimize the system directly. Unfortunately, this algorithm will not work in this FT reactive distillation case study, simply because the system will not be able to converge with all of its 30 thousand variables randomized.

Principally, not all variables are required to be randomized in order for multi-start to work since most of them are directly correlated. In contrast, multi-start should be most effective when the system is only randomly initialized within the feasible subspace. However, as we have discussed above, the feasibility region for this problem is difficult to define. As a result, we propose a multi-start algorithm that randomly initializes within the operability subspace, which shares the same dimension as feasible subspace, but is larger and contains the feasible subspace.

1. Remove complicating constraints such as quality constraints or adiabatic constraints.
2. Generate a list of “Non-basic” variables to be used as multi-start variables
3. Multi-start “Non-basic” variables by randomly assigning value
4. Because values for those variables are set (Such as temperature), sequential initialization strategy can be applied and generate a solution that is close the feasibility.
5. Add constraints back, resolve

The following is a list of variables and their distributions in the operability region:

Variable	Initialization Value	Distribution
Distillate ratio	[0.05,0.15]	Uniform
Heavy naphtha location	[1,2]	Random integers
Heavy naphtha draw %	[0.01,0.03]	Uniform
Gasoline location	[3,9]	Random integers
Gasoline draw %	[0.1,0.3]	Uniform

Variable	Initialization Value	Distribution
Diesel location	[10,18]	Random integers
Diesel draw %	[0.2,0.5]	Uniform
Temperature	[220,280]	Uniform and sorted
Catalyst	[100,30000]	Uniform and normalized
Feed	[0.01,10]	Uniform and normalized

Note that the product draw % is not one of the column configuration constraints but are necessary to fully define the system. The percentage here is chosen based on experience. Also, note that the temperature is set to be smaller than allowable range, based on experience. As can be seen from the reactive flash case study, the optimum temperature for gasoline production falls within 220C to 280C, narrowing the range down will generate initializations that are closer to optimum solution.

In this case study, for reproducibility and model validation purposes, 1000 sets of randomly initialized variables are generated and saved. We will be referring to them as case 1-1000 in the discussion.

2.4 Optimization

After initialization, the optimization of a FT reactive distillation column will be done in four steps. First, the model is transformed by introducing Differentiable Distribution Function (DDF) to replace discrete decision variables, such as product tray and reflux location.

$$P_{tray,p} = LP_p \cdot \frac{e^{-\frac{(i-N_{tray})^2}{\sigma}}}{\sum_j e^{-\frac{(j-N_{tray})^2}{\sigma}}} \qquad \forall i$$

Second, the model is relaxed and optimized using a revenue-based objective such as total product revenue, with an emphasis on gasoline production. Third, the model is relaxed further and optimized using a profit-based objective, with the addition of cost functions such as feed gas and total tray count.

Globalization strategy will be applied to the 2nd step, where the most computational work will take place. All the computational work is done through Amazon Web Service (AWS)'s c4.8xlarge instance with 36 Intel Xeon E5-2666 v3 2.9GHz cores and 60Gb memory. A custom Amazon Machine Image (AMI) is created for this case study, fully configured with the Ipopt-3.12.11 and HSL linear solver ma97.

While it is tempting to apply globalization strategy to the 3rd step as well, in practice however, this step typically only involves proportional change in stage feed flow, as well as shift of reflux tray location. Therefore, we believe that the transition from 2nd step to 3rd step is smooth and will not change the overall solution model structure. As a result, 3rd step will be applied directly to any successfully solved 2nd step cases during globalization.

There are two cost components to 3rd step optimization, one is the total tray count, the other is total feed cost. These two components are heavily correlated. For example, a high tray cost would lead to lower total tray count, which decreases feed utilization, resulting in less total feed in optimum solution. Within their respective range, the effects of these two components could result in one dominating the other. In this case study, we will show three 3rd step optimization cases with different weights, to illustrate different optimum solutions when the cost is different.

A list of relaxed variables and their respective bounds.

Variable	Bounds – Step 2	Bounds – Step 3
Distillate Ratio	$[0.05,1]$	Same as Step 2
Heavy Naphtha Flow	$[0,\infty]$	
Heavy Naphtha Location	$[1,2]$	
Gasoline Flow	$[0,\infty]$	
Gasoline Location	$[3,9]$	
Diesel Flow	$[0,\infty]$	
Diesel Location	$[10,18]$	
Temperature (Reactive)	$[200,300]$	
Catalyst	$[100,30000]$	
Feed	$[0.01,10]$	
Reflux Tray Location	Fixed	$[1,5]$
Bottom Feed Location		$[15,20]$
Total Feed		$[1,\infty]$

A list of objective weights.

Step	C1-C4 & Gas	Naphtha	Heavy Naphtha	Gasoline	Diesel	Heavy	Tray	Feed
2	N/A	43	20	90	128	100	N/A	N/A
3	1.3	43	20	90	128	100	-0.005	-2.24
3-1	1.3	43	20	90	128	100	-0.4	-2.24
3-2	1.3	43	20	90	128	100	-0.005	-1.9

3 Results and Discussion

3.1 Success Rate

Out of the 1000 randomly initialized samples, 5 of them freezes during solve and have to be terminated without logs. The others are categorized into the following table:

Category	Number	Step success rate	Overall success rate
Total Runs	995	-	-
Initialized	899	90.35%	-
Product DDF	880	97.89%	88.44%
Revenue Optimum	564	64.10%	56.68%
Tray DDF	564	100%	56.68%
Profit Optimum			
3	562	99.65%	56.48%
3-1	550	97.52%	55.28%
3-2	552	97.87%	55.48%

As excepted, two areas contribute to most of the failure cases are initialization and the first optimization step.

3.1.1 Initialization

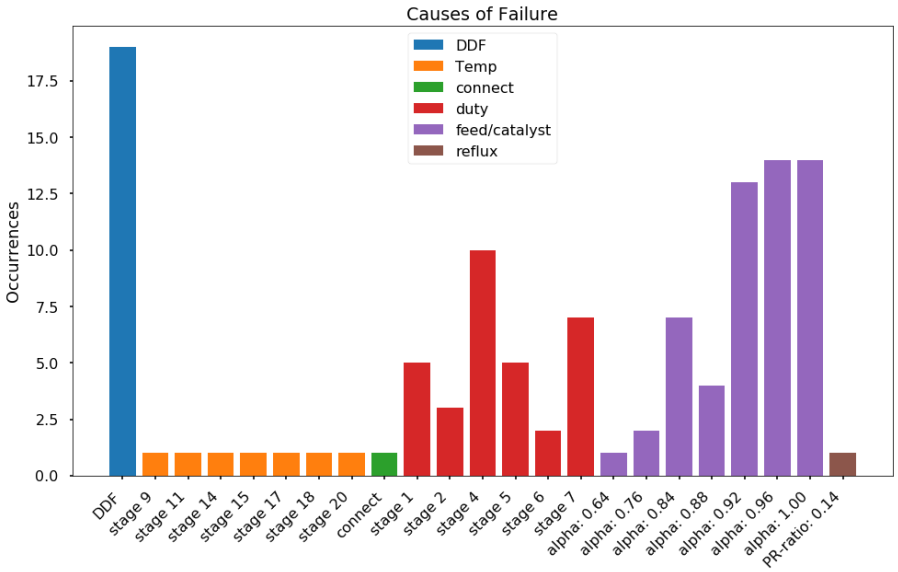

A few remarks about breakdown of the step during which initialization failure occurs:

1. Adjusting feed / catalyst is done by simultaneous changing their respective values from the baseline, using an iterative changeover ratio α. As shown in the histogram above, chance of failure increases with increase in α. Our hypothesis is that some randomized feed / catalyst profiles give rise to disappearing liquid conditions

described above. Moreover, to cover the entire operability region, the range of feed / catalyst covers throughout its lower and upper bound, this gives occasionally weird profiles. As a result, the system becomes extremely difficult to solve and often runs out of iterations.

2. DDF reformulation on product extraction tray is the single highest failure cause, due to scaling issues associated with distribution equation when calculating trays that are far away from the mean tray. The fact that various product extraction overlaps each other also increased the challenge. As discussed in the package report, the equations are modified to keep a minimum flow, as well as solver haustra's are incorporated for better linear system scaling. Despite these efforts, the DDF formulation is a major cause of failure.
3. Heat duty step means the transition of a stage to adiabatic. Usually, a large shift in temperature is associated with such change. As a result, this step is prone to failure as the change in temperature causes difficulties in resolving VLE equations.
4. Various single failures occurred during reflux, temperature adjustment, and the initial column construction connected solve. These have no specific causes and are mostly likely incidents related to solver.

Overall, since the parameters are entirely randomly generated, it is expected to have certain number of unsolvable cases. We are overall very satisfied with larger than 90% success rate.

3.1.2 Optimization

Category	Failure Cause	Number
Revenue (First optimization step)	Maximum Number of Iterations Exceeded	304
	Restoration Failed	11
	Converged to a point of local infeasibility	1
Profit		
3	Maximum Number of Iterations Exceeded	2
3-1	Maximum Number of Iterations Exceeded	14
3-2	Maximum Number of Iterations Exceeded	11
	Restoration Failed	1

Optimization failure subject to multiple aspects and is very hard to analyze what the root cause is. Sometimes it could simply be the bad start point, which is inevitable in randomized multi-start setting. Among all failures, some of the restoration failure are worth noting.

3.1.3 Improving Optimization Success Rates

After an overview of success rates per optimization step, we now turn our attention to the success rates' distribution with different values of starting point. The following list of graphs will show two key statistics of this study: 1) the parameter distribution (x-axis) of chosen initial starting point by the number of total cases (y-axis). 2) the success rate within that range.

The graphs are enlarged for easy viewing.

A few remarks about the distribution of initial start point and optimization success rates:

1. Low initial reflux ratio has low optimization success rate. This is consistent with the fact that product quality is not satisfied during initialization. Therefore, for the final optimum solution to satisfy quality constraints, the reflux ratio is required to be high. Therefore, low initial reflux ratio has similar initialization success rate, but low optimization success rate.

2. High diesel product tray has low optimization success rate. This is consistent with the final optimum result. In this case study, for most optimum cases, the diesel extraction tray sits above catalyst section. As we all know catalyst section produces wide range of products, and thus is not possible to become product tray. Therefore, if the initial point has the diesel extraction below bulk catalyst tray, it could be difficult to move it across.
3. Success rates for temperature, catalyst and feed distribution is stable throughout all regions. The fluctuations shown in the graphs are primarily due to low sample sizes. Since feed and catalyst are normalized to a fixed total amount, the sample sizes for extremely large feed and catalyst is rare, thus the success rates for those cases could be fluctuating. Interestingly, most extreme cases produce high success rate. This could suggest that a dominant feed / catalyst profile is close to a local minimum and thus easy to optimize.

To visualize the distribution of randomized features and success rates. A PCA with 2 principle components is plotted.

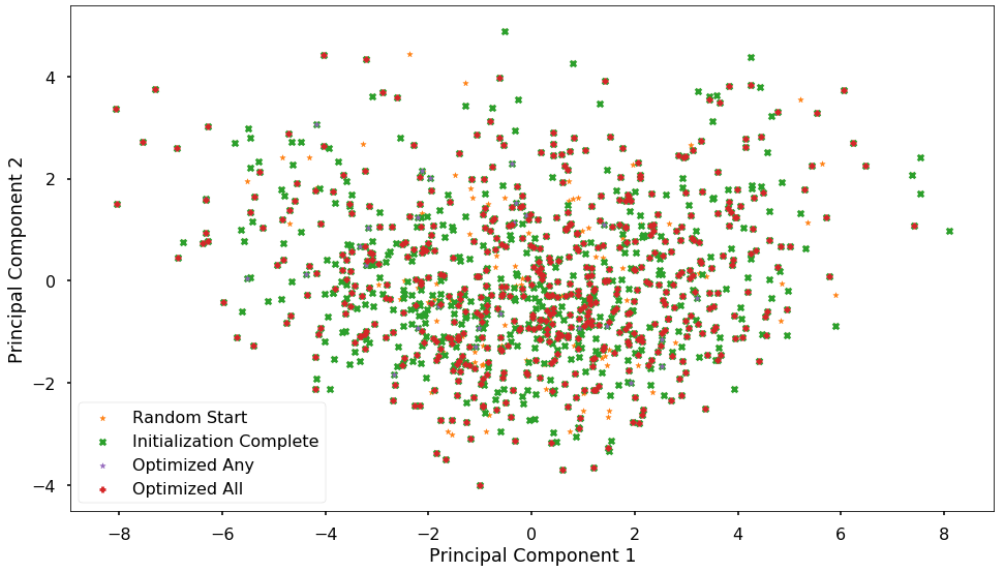

While most of the projection on PC1 and PC2 plane reveals that the majority of the success rates for cases are eventually distributed, we do find a that a high negative PC1 score favors high optimization success rate, while a high positive PC1 score favors low optimization success rate. If we plot the loading for PC1, we will find that PC1 mostly shows that temperature

is heavily correlated, since temperature is sorted to reflect normal operating condition. Apart from that, all other variables are independent of each other, and thus shows little correlations.

Based on this, a high PC1 score is definitely the result of overall high temperature, and a low PC1 score is the result of overall low temperature. As can be seen from optimization result, to favor gasoline and diesel production, the optimum temperature is in the lower end of the operation range. Therefore, it makes sense that an overall low temperature favors success rates, since it is closer to the optimum solution.

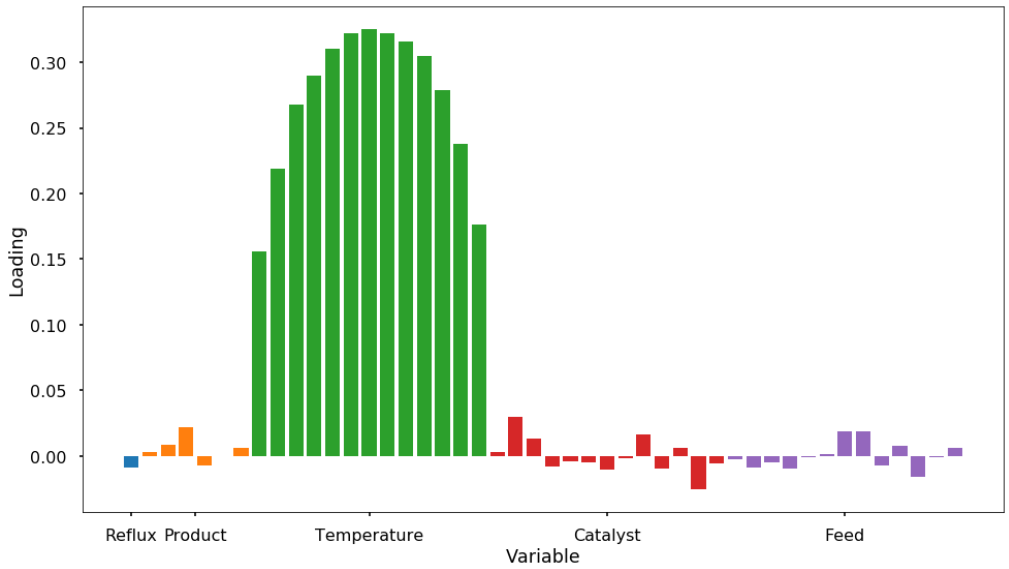

To summarize, the operation parameters used to initialize the reactive distillation column doesn't seem to be biased towards the overall success rates of both initialization and optimization. There are specific extremes that tie into high failure rates and that leads to our recommendation for initialization parameters that could improve optimization success rate:

1. Initialize with high reflux ratio
2. Initialize with product tray at appropriate position. For example, diesel tray close to the middle section, rather than bottom section
3. Initialize with low temperature

3.2 Optimization Statistics

3.2.1 Revenue

As expected, a highly non-linear system such as the FT reactive distillation column has a large number of local minimums. Among 564 successfully solved cases, a total of 394 unique local minimums are discovered. Their distribution is shown in a histogram below:

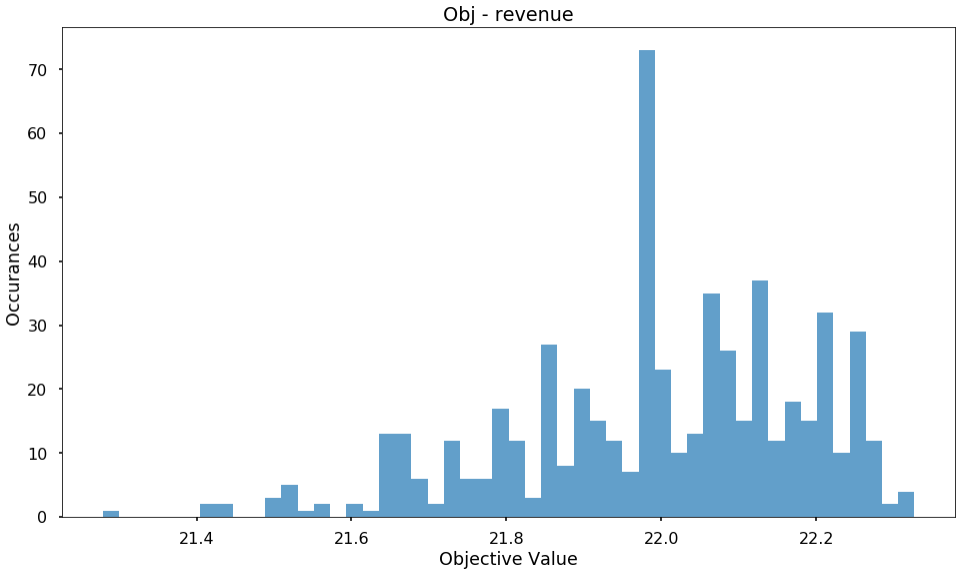

As discussed before, the system is fully defined by the 46 operating variables as degrees of freedom. Therefore, we will decompose all 46 different features using PCA on all unique local minimums. First, we will focus on the relationship between objective value and their feature sets, find out how the objective change as features change. Second, we will study the relationship between optimum objective and their initial feature sets, find out what kind of initialization leads to the best objective. For convenience, we categorize solutions as follows.

Notation	Cut-off Case Number	Cut-off Objective
"Bad"	100	21.888
"Middle"	250	22.114
"Good"	350	22.228
"Super"	394	22.327

PC	Eigenvalue	Explained Variance
1	7.49	17.4%
2	4.71	10.9%
3	3.04	7.04%
4	2.29	5.32%
5	2.10	4.88%

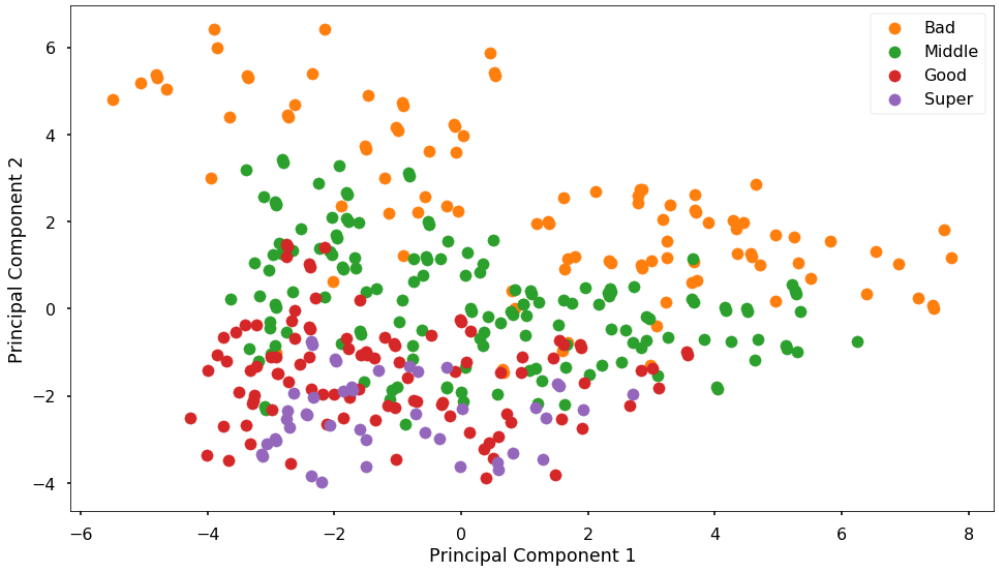

The graph above is a 2-D plot of PC1 and PC2 with regards to different classes of objective values we just defined early. Note that each dot represents a unique local minimum. Imagine that in this system, each local minimum is a small hill located on a much larger sloped ridge. As a result, not only will this map suitable for predicting local optimums, but also suitable to predict the general objective value given principal components.

Immediately we see a sharp separation between different classes. Surprisingly we see that representations from each class distribute throughout the range of PC1. We believe that PC1 captures mostly minor shift in design, which gets amplified by internal negative correlation between similar features, due to their summation constraint. For example, two designs with catalyst concentrating in adjacent trays could easily have similar objectives. However, since the sum of catalyst is the same, the negative correlation determines that they will have opposite scores. After PC1 filers out design differences, PC2 could show us more generic details in what kind of fine-tuning a design needs to have to achieve high objectives.

3.2.1.1 PC1 – Design Shift

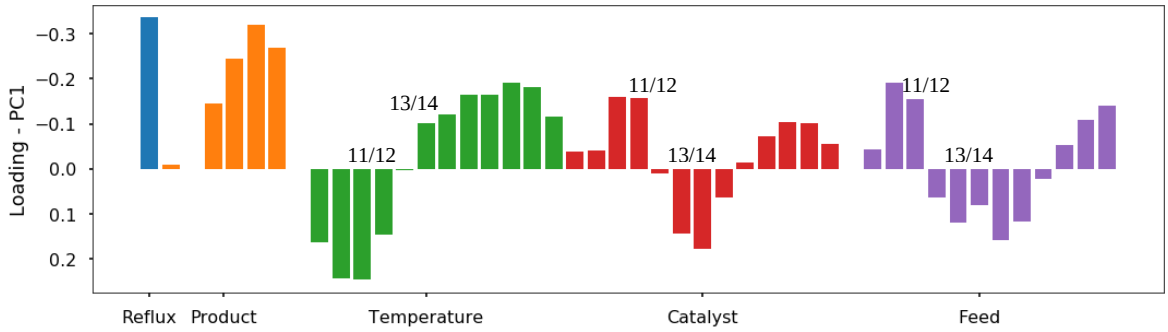

Looking at the PC1's loading diagram, as expected, variables have negative correlations within different trays. As a result, even similarly designed columns could have opposite scores. Here we will pick 2 best cases from positive and negative PC1 values to illustrate the point.

As can be seen from below, the two cases are extremely similar to each other, they only differ from each other in terms of Tray 11 / 12 and Tray 13 / 14.

Case	Objective	PC1	Non-reactive	Reactive	
63	22.327	+1.18	11 / 12	13 / 14	Positive by catalyst and feed
307	22.324	-1.72	13 / 14	11 / 12	Negative by catalyst and feed

In short, a reactive tray cannot become a product extraction tray due to low product quality. As a result, in some cases non-reactive trays are inserted in the middle to create extraction points that satisfy product quality. In the two cases below, the only difference is the choice of those non-reactive tray location.

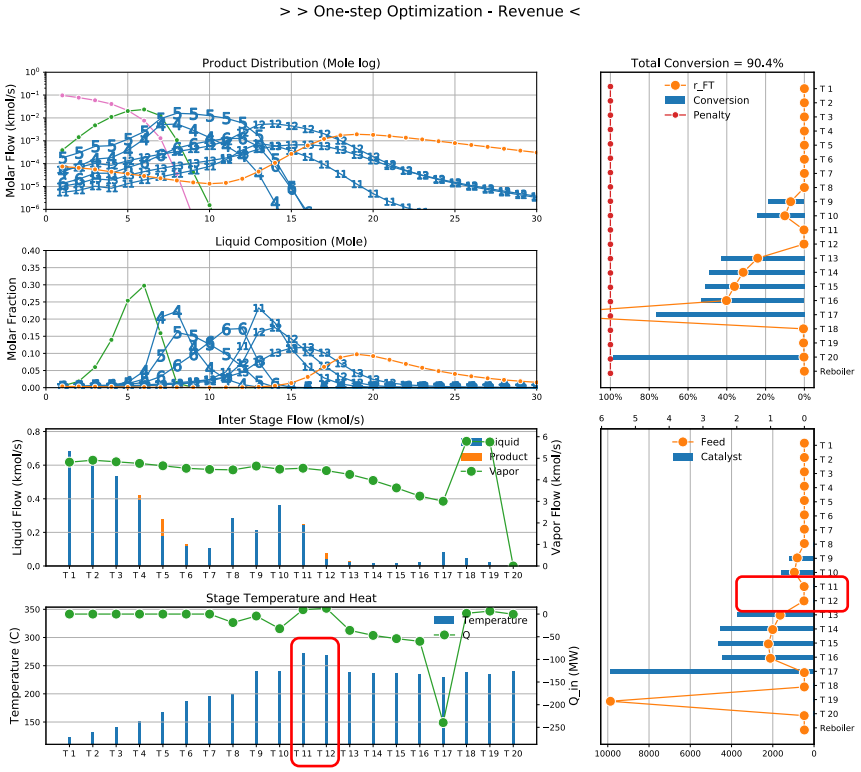

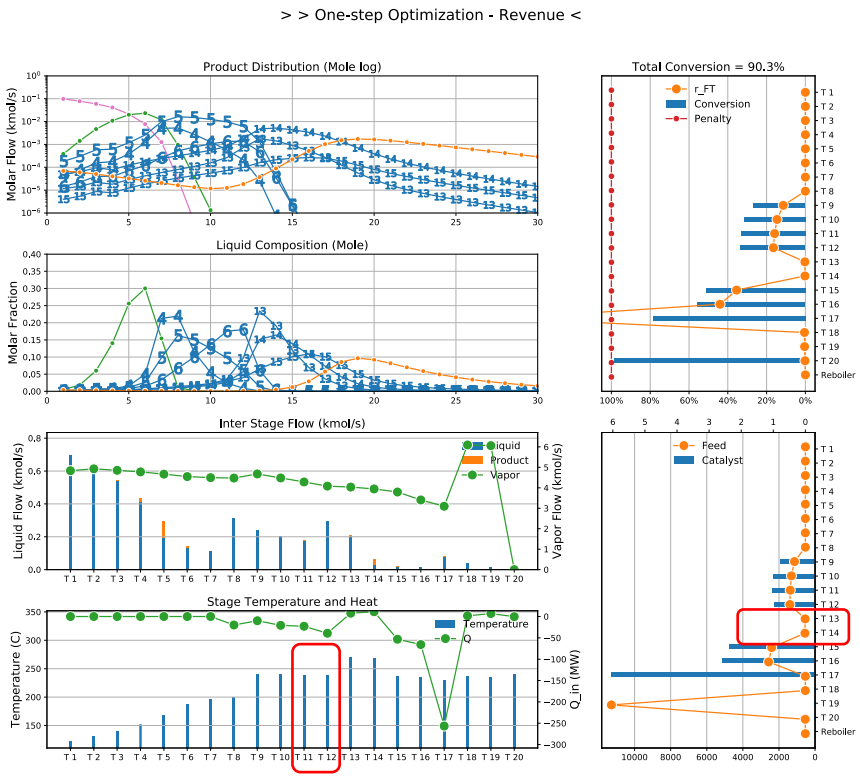

3.2.1.2 PC2 – Increasing Objective

After PC1 filters out internal negative colorations caused by summation constraint, PC2 is able to capture a design loading vector that shows a strong connection to the final objective.

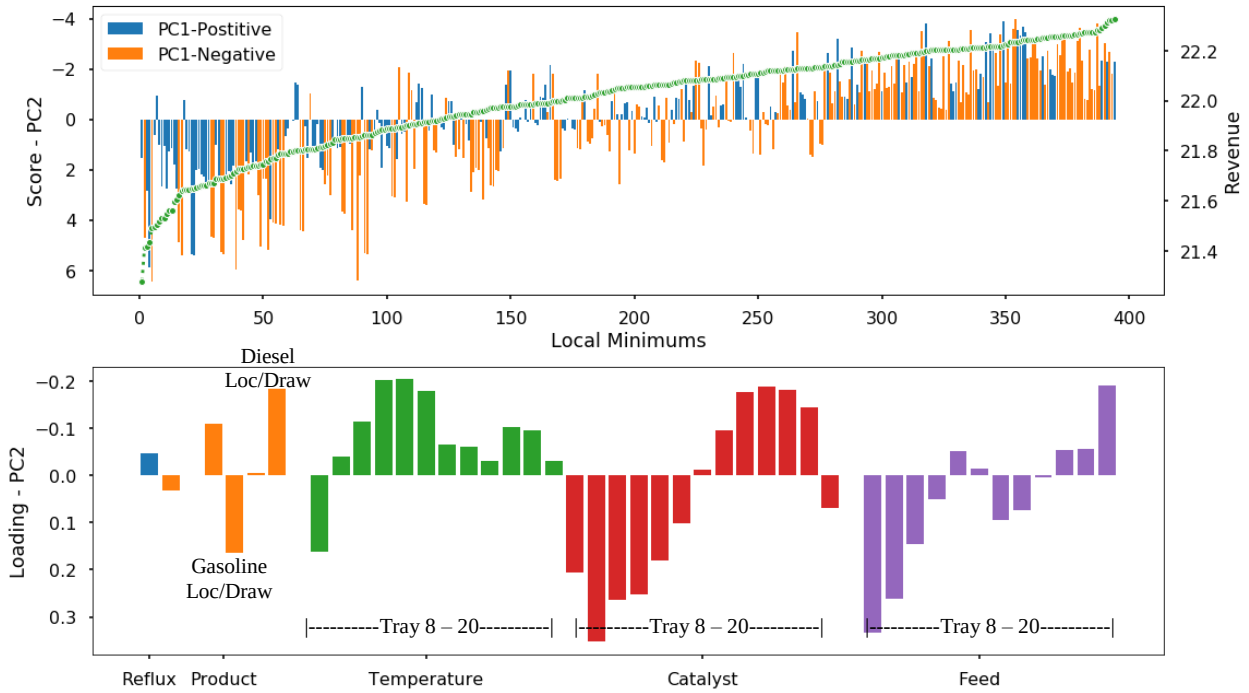

As can be seen from the figure, both PC1 positive and negative cases are distributed eventually throughout the sorted x-axis. This further supports the fact that PC1 only captures internal negative correlation and is not biased towards better or worse objective.

By plotting the total revenue against PC2 score, we can see a clear correlation between them. While the middle section is open to interpretation, the left and right portion of the plot is indisputably showing that the PC2 loading vector direction is favoring higher revenue objective.

The PC2 loading vector can be interpreted as follows and is consistent with our understanding of the reactive distillation system.

Beneficial Feature Vector	Notes
High gasoline tray More gasoline product Less diesel product	Economic Value of gasoline is higher
Higher temperature at reactive section	Higher temperature promotes reaction and gasoline production
Less catalyst at upper reactive section More catalyst at lower reactive section	Promotes better separation, especially for diesel product
Less feed at upper section More feed at lower section	Feed stripping

3.2.1.3 Dependency on initialization

After a strong dependency between optimized feature set and objective value has been found, its dependency on initialization has been studied as well. In the graph below, we apply the original mean-center, normalize and dimension reduction matrix to each sample's initial starting point.

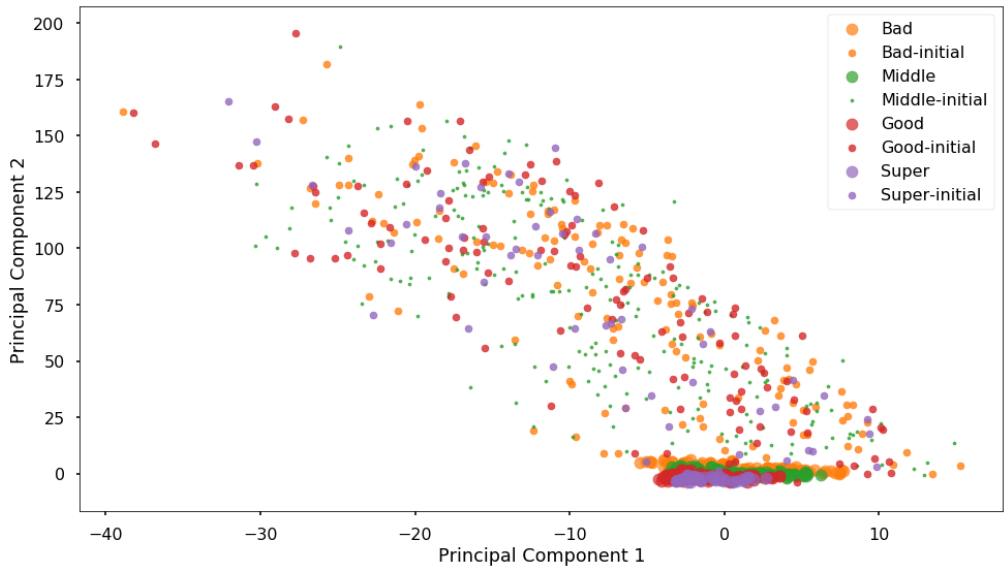

So far, we cannot find and direct relationship between the initial start point and the final optimized solution. Non-linear optimization is a complicated process and the fact that initial starting point doesn't correlate to where the optimizer would end up is reasonable. This also means that for this certain objective, a random start that could cover the entire operability region is essential to find the optimum solution. It is worth noting that this is not always the case, for the profit objective in section 3.3, we can show a very separable relationship between initialization and final solution, which means that multi-start region can be further optimized.

3.3 Profit

The statistical analysis for profit follows the similar structure as revenue optimization. Discussion will be omitted here but key graphs are attached for reference.

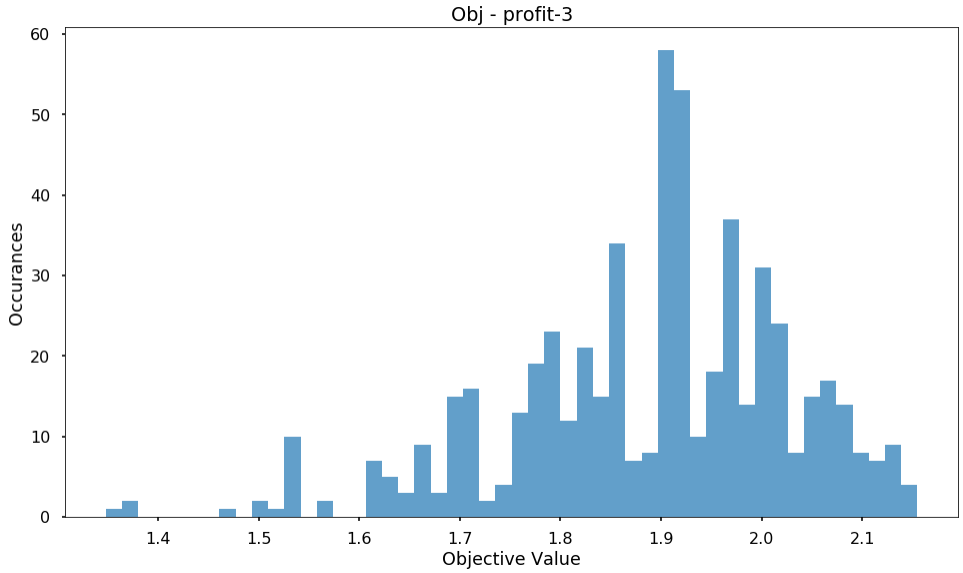

Notation	Cut-off Case Number	Cut-off Objective
“Bad”	100	1.837
“Middle”	200	1.953
“Good”	300	2.043
“Super”	349	2.155

PC	Eigenvalue	Explained Variance
1	8.46	18.7%
2	6.26	13.9%
3	3.31	7.34%
4	2.59	5.74%
5	2.43	5.39%

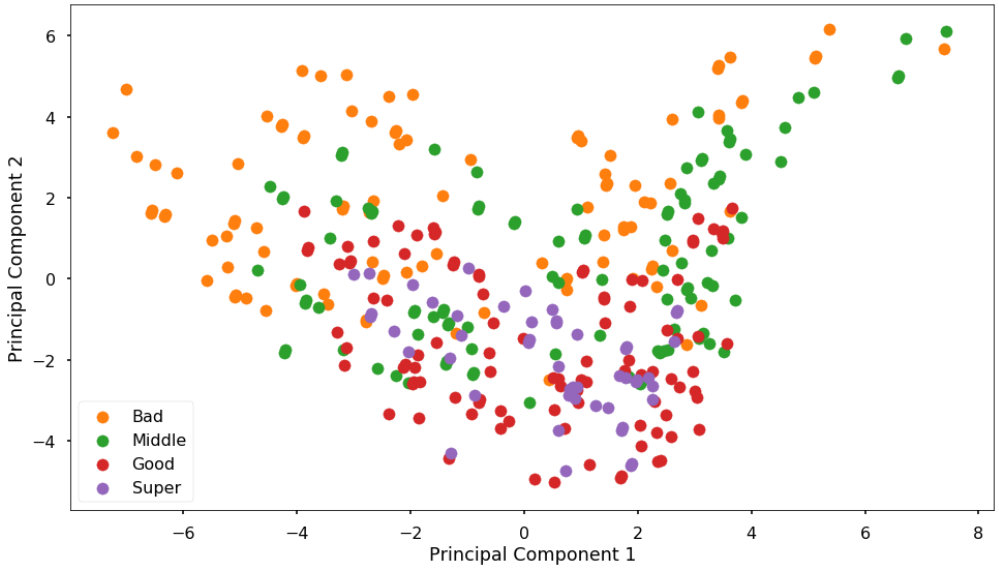

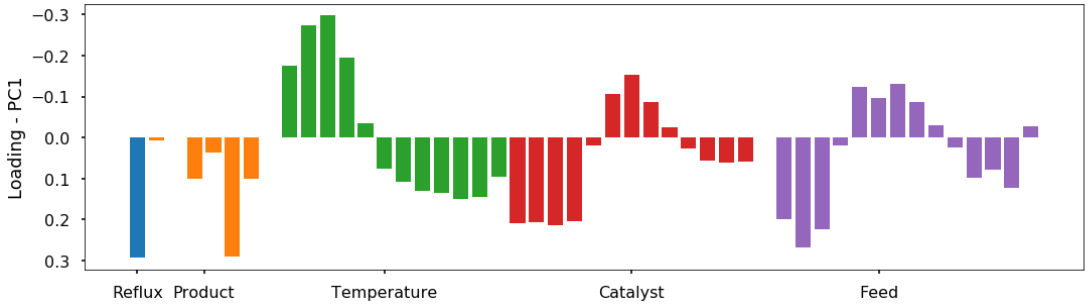

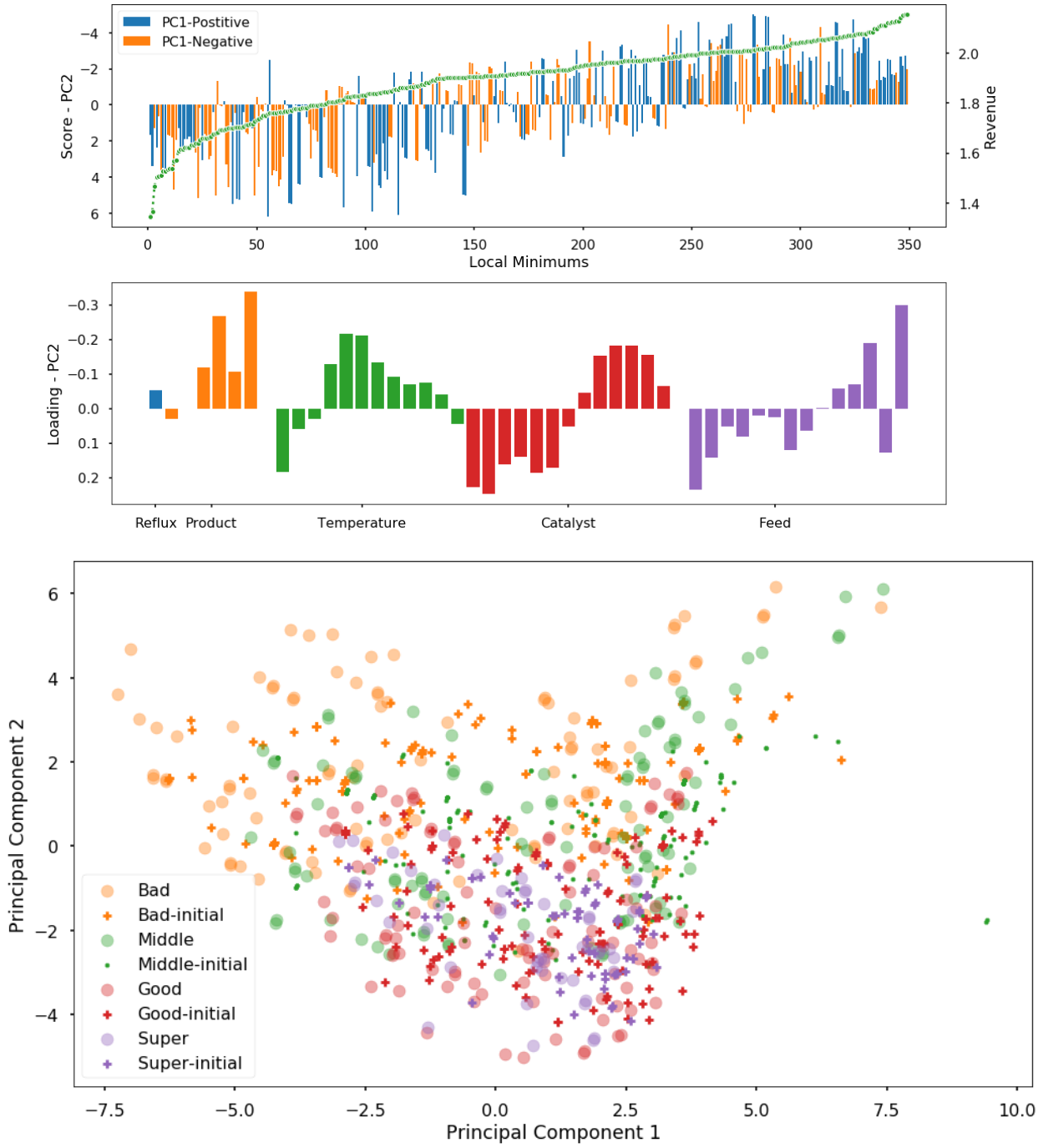

Note that in this study, we hypothesize that the globalization strategy only needs to be applied to the first optimization step, reduced multi-start, and that subsequent steps will only be fine tuning. As shown from the graph above, the optimization step doesn't take the optimum solution far away from the initial solution. Based on this, we can postulate that, if we only apply multi-start at the purple / red region, the chances of finding higher objectives will be higher.

3.4 Optimum Results

Since there are hundreds of local optimums, here we will first only pick only the global optimum and explain some of its optimum features. Next, we will conduct a sensitivity test on the global optimum and explain how the different economic objective influences design choices. Finally, we will solve the same optimization problem using a FT reactive flash and discuss why a FT reactive distillation column outperforms the reactive flash.

3.4.1 Revenue Best Case (Case: 63, Obj: 22.327, Conv = 90.37%)

stages	T	Q					V	L	P	W
condenser	30	-149					1.6597	0.5903	0.0787	2.4905
stages	T	Q	r_FT	Con%	F	cat	V	L	P	P_{VLE}
NON--[1]	122.7	0	0	0	0	0	4.819	0.680	0	20
NON--[2]	131.3	0	0	0	0	0	4.909	0.607	0	20
NON--[3]	140.6	0	0	0	0	0	4.836	0.531	0.000	20
NON--[4]	152.2	0	0	0	0	0	4.760	0.398	0.024	20
NON--[5]	168.4	0	0	0	0	0	4.651	0.181	0.099	20
NON--[6]	186.8	0	0	0	0	0	4.533	0.122	0.007	20
NON--[7]	196.0	0	0	0	0	0	4.482	0.101	0	20
React[8]	200.0	-18.6	0	0	0.00	10	4.461	0.280	0	20
React[9]	239.4	-4.3	0.070	0.185	0.21	1185	4.639	0.210	0	20
React[10]	240.2	-32.2	0.100	0.243	0.29	1566	4.493	0.360	0	20
React[11]	272.1	9.7	0.002	0.007	0.01	10	4.538	0.248	0.003	20
React[12]	269.0	12.8	0.001	0.006	0.01	10	4.426	0.047	0.031	20
React[13]	238.8	-35.9	0.241	0.431	0.72	3694	4.249	0.022	0.006	20
React[14]	237.5	-47.0	0.315	0.491	0.94	4538	3.969	0.017	0	20
React[15]	236.3	-54.1	0.360	0.514	1.07	4627	3.624	0.017	0	20
React[16]	235.1	-60.1	0.401	0.530	1.01	4435	3.243	0.020	0	20
React[17]	229.8	-239.0	1.420	0.766	0.00	9849	3.004	0.083	0	20
React[18]	238.6	1.7	0.004	0.003	0.00	10	5.787	0.042	0	20
React[19]	235.3	6.6	0.004	0.002	5.74	10	5.755	0.018	0	20
React[20]	240.2	-0.4	0.002	0.984	0.01	52.85	0.000	0.021	0	20
stages	T	Q					V	L	P	P_{VLE}
reboiler	350	1.938					0.0016	0.0197	20	
naphtha	:	0.75	Wet	:	0.0787	Dry	:	N_tray	:	0
gasoline	:	0.75	Wet	:	0.1309	Dry	:	N_tray	:	4.8
diesel	:	0.75	Wet	:	0.0406	Dry	:	N_tray	:	12.1
heavy	:	0.75	Wet	:	0.0197	Dry	:	N_tray	:	21
intermediate	:	1	Wet	:	0.0002	Dry	:	N_tray	:	2

A few important features can be observed from the best revenue case:

1. Feed stripping is used heavily in the solution. More than half of the feed enters the system at stage 19, while the rest is fed as make-up gas throughout reactive stages.
2. Reactive section is divided into 2 parts. The bulk of the reaction happens from stage 13 to stage 17, while stage 9 and 10 acts as gatekeeper to maximize overall conversion.

3. The middle of the reactive section is left out as non-reactive stage in order for the product diesel to satisfy quality constraint. As a result, diesel extraction point is constrained within this region and gasoline tray is optimized accordingly.
4. Reactive section's temperature is reversely ordered, with higher temperature at top stages. One explanation for this behavior is that high temperature produces lighter hydrocarbon. Therefore, in a way, the arrangement of the stage itself is helping out the separation.

When this case is subject to further optimization, the following results are obtained:

Step	C1-C4	Naphtha	Heavy Naphtha	Gasoline	Diesel	Heavy	Tray	Feed
Revenue	N/A	43	20	90	128	100	N/A	N/A
Profit	1.3	43	20	90	128	100	-0.005	-2.24
3-1	1.3	43	20	90	128	100	-0.4	-2.24
3-2	1.3	43	20	90	128	100	-0.005	-1.9

	Revenue		Profit		3-1		3-2	
	Conversion	Reflux Ratio	Conversion	Reflux Ratio	Conversion	Reflux Ratio	Conversion	Reflux Ratio
	90.37%	7.50	90.60%	7.56	89.77%	8.33	87.56%	7.60
	Flow (kmol/s)	Quality	Flow (kmol/s)	Quality	Flow (kmol/s)	Quality	Flow (kmol/s)	Quality
Naphtha (C5 – C7)	0.0787	0.75	0.0703	0.75	0.0624	0.75	0.1229	0.75
Gasoline (C8 – C12)	0.1309	0.75	0.1196	0.75	0.1114	0.75	0.1909	0.75
Diesel (C13 – C18)	0.0406	0.75	0.0379	0.75	0.0378	0.75	0.0586	0.75
Heavy (C19 – C56)	0.0197	0.75	0.0193	0.75	0.0219	0.75	0.0198	0.75
Heavy Naphtha	0.0002	1	0.0002	1	0.0002	1	0.0002	1
	Product Tray	Reflux Tray	Product Tray	Reflux Tray	Product Tray	Reflux Tray	Product Tray	Reflux Tray
Naphtha (C5 – C7)	0	1	0	1.000	0	3.635	0	1.034
Gasoline (C8 – C12)	4.8	Total Feed	4.8	Total Feed	6	Total Feed	3.8	Total Feed
Diesel (C13 – C18)	12.1	10	12.1	9.089	12.6	8.921	12.9	15.770
Heavy (C19 – C56)	21	Obj	21	Obj	21	Obj	21	Obj
Heavy Naphtha	2	22.328	2	2.128	2	2.773	2	6.272
	Feed (kmol/s)	Catalyst (kg)	Feed (kmol/s)	Catalyst (kg)	Feed (kmol/s)	Catalyst (kg)	Feed (kmol/s)	Catalyst (kg)
React[8]	0.001	10	0.001	10	0.001	57.36	0.001	10
React[9]	0.21	1185	0.001	33.75	0.001	51.92	0.75	2744
React[10]	0.294	1566	0.001	10	0.001	10.03	0.883	3046
React[11]	0.006	10	0.006	10	0.003	10	0.003	10
React[12]	0.011	10	0.009	10	0.001	10	0.022	10

	Revenue		Profit		3-1		3-2	
React[13]	0.717	3694	0.472	2830	0.013	10	1.287	4026
React[14]	0.937	4538	0.785	4530	0.529	3258	1.574	4681
React[15]	1.066	4627	0.959	4969	0.828	4694	1.698	4584
React[16]	1.006	4435	1.032	5125	1.002	5521	1.267	4007
React[17]	0.001	9849	0.001	12379	0.001	16266	0.001	5119
React[18]	0.001	10	0.001	10	0.001	10	0.001	10
React[19]	5.738	10	5.812	10	6.529	10	8.273	1715
React[20]	0.005	52.85	0.006	70.72	0.006	89.75	0.005	34.72
	Temperature	Liquid (kmol/s)	Temperature	Liquid (kmol/s)	Temperature	Liquid (kmol/s)	Temperature	Liquid (kmol/s)
React[8]	200	0.2798	200	0.2156	200	0.2017	200	0.5328
React[9]	239.4	0.2104	233.2	0.3064	225.4	0.2635	243.9	0.406
React[10]	240.2	0.3599	258.6	0.3303	246.7	0.3065	243.6	0.5485
React[11]	272.1	0.2475	272.6	0.2242	263.5	0.2574	264.6	0.4935
React[12]	269	0.0465	267.4	0.0396	266.3	0.1558	269.3	0.1943
React[13]	238.8	0.0221	237.4	0.0171	261.8	0.0186	243.1	0.0818
React[14]	237.5	0.0168	236.4	0.0133	234.5	0.0115	241	0.0445
React[15]	236.3	0.0172	235.7	0.0145	234.4	0.0122	239.2	0.034
React[16]	235.1	0.0201	234.9	0.0179	233.9	0.0157	237.4	0.0337
React[17]	229.8	0.0826	230.3	0.0899	229.1	0.1082	233.5	0.0664
React[18]	238.6	0.0423	239.6	0.0433	241.1	0.0497	241	0.0342
React[19]	235.3	0.018	236.1	0.0177	237	0.02	232.2	0.0184
React[20]	240.2	0.0212	236.1	0.0211	233.4	0.024	245.4	0.0212

There is a lot information to be covered here, we will divide them by transitions of objective.

3.4.1.1 Revenue → Profit

When the objective changes from revenue to profit, the system begins to optimize its total feed and reflux tray location. Total feed and reflux tray location has a negative coloration simply because increased value in one will suppress the other. For example, an increase in reflux tray means the system capacity is suppressed in favor of reduced cost. Therefore, feed would be reduced accordingly to minimize waste. We will see more example when we discuss case 3-1 and 3-2.

In the case of revenue → profit, we see that given the cost of trays and feed, the system decides to reduce feed while keeping the reflux tray at 1. This shows that the original design is an under-designed system that takes too much feed. As a result of reduced feed, the upper

reactive "gatekeeper" section is not necessary anymore, as indicated by the reduced catalyst loading.

3.4.1.2 High Tray Cost (3-1)

Recall that to transit from original profit objective to 3-1, we increase the weight of trays to simulate an increased interest in reducing total tray count. After optimization, reflux tray location is increased to 3.635. As expected, this move reduces the overall system capacity, thus the optimum feed amount is further reduced from 9.089 to 8.921 (10 in revenue optimization).

In addition to reduced feed, other system variables are optimized to compensate reduced overall capacity. The reflux ratio is increased from 7.56 to 8.33 to improve rectifying section performance. The bottom feed is also increased from 64% total feed to 73% total feed to improve stripping performance.

3.4.1.3 Low Feed Cost (3-2)

A reduced feed cost motivates the system to process as much as feed as possible, while paying less to economic objective like waste. The optimum solution features an increased feed of 15.77, a 50% increase from the original value. As expected, the overall conversion drops from about 90% to 87.5%.

Increased feed also prompts the return of upper reactive "gatekeeper" section. In the optimum solution, we see the section features almost double the original section, indicating that more feed gas escapes the major reactive section and thus have to be consumed in the upper section.

3.4.2 Profit Best Case (Case: 317, Obj: 2.155, Conv = 90.65%)

Interestingly, the best profit optimization solution does not come directly from the best case for revenue optimization. In our study, subsequent optimization case warm starts from the first optimum and it is reasonable to assume that the solution structure will remain similar. Therefore, the best solution structure for revenue optimization may not be the same for profit optimization. As a result, we have another optimum that maximizes profit.

	Revenue		Profit		3-1		3-2	
	Conversion	Reflux Ratio	Conversion	Reflux Ratio	Conversion	Reflux Ratio	Conversion	Reflux Ratio
	90.36%	7.61	90.65%	7.73	89.72%	8.88	87.60%	7.60
	Flow (kmol/s)	Quality	Flow (kmol/s)	Quality	Flow (kmol/s)	Quality	Flow (kmol/s)	Quality
Naphtha (C5 – C7)	0.0783	0.75	0.0679	0.75	0.0569	0.75	0.1222	0.75
Gasoline (C8 – C12)	0.1309	0.75	0.1172	0.75	0.1057	0.75	0.1897	0.75

Diesel (C13 – C18)	0.0408	0.75	0.038	0.75	0.0375	0.75	0.0584	0.75
Heavy (C19 – C56)	0.0193	0.75	0.0185	0.75	0.0213	0.75	0.0195	0.75
Heavy Naphtha	0.0002	1	0.0002	1	0.0002	1	0.0002	1
	Product Tray	Reflux Tray	Product Tray	Reflux Tray	Product Tray	Reflux Tray	Product Tray	Reflux Tray
Naphtha (C5 – C7)	0	1	0	1.000	0	3.908	0	1.042
Gasoline (C8 – C12)	4.9	Total Feed	4.8	Total Feed	6.1	Total Feed	3.8	Total Feed
Diesel (C13 – C18)	12.9	10	13	8.878	13.9	8.518	12.8	15.659
Heavy (C19 – C56)	21	Obj	21	Obj	21	Obj	21	Obj
Heavy Naphtha	2	22.313	2	2.155	2	2.848	2	6.241
	Feed (kmol/s)	Catalyst (kg)	Feed (kmol/s)	Catalyst (kg)	Feed (kmol/s)	Catalyst (kg)	Feed (kmol/s)	Catalyst (kg)
React[8]	0.001	10	0.001	10	0.001	10	0.001	10
React[9]	0.235	1332	0.088	581.6	0.001	39.48	0.774	2870
React[10]	0.004	10	0.001	10	0.001	28.51	0.009	10
React[11]	0.367	1882	0.002	10	0.001	10	0.98	3312
React[12]	0.317	1501	0.006	10	0.002	10	1.055	3357
React[13]	0.013	10	0.007	10	0.006	10	0.013	10
React[14]	0.864	4257	0.755	4590	0.01	10	1.613	4858
React[15]	1.106	4999	1.024	5658	0.668	4138	1.711	4656
React[16]	1.111	4991	1.125	5826	1.096	6692	1.288	4039
React[17]	0.001	10934	0.001	13207	0.001	18943	0.001	5099
React[18]	0.001	10	0.001	10	0.001	10	0.001	10
React[19]	5.969	10	5.856	10	6.721	10	8.203	1731
React[20]	0.005	51.79	0.005	66.03	0.007	87.48	0.005	34.21
	Temperature	Liquid (kmol/s)	Temperature	Liquid (kmol/s)	Temperature	Liquid (kmol/s)	Temperature	Liquid (kmol/s)
React[8]	200	0.2986	200	0.2489	200	0.1731	200	0.5332
React[9]	239.5	0.3057	236.9	0.2674	217.4	0.2002	243.8	0.5229
React[10]	251.5	0.1929	250.3	0.2979	231.2	0.242	254.2	0.3427
React[11]	240.4	0.1656	262.8	0.2986	246.2	0.2747	243.6	0.276
React[12]	241.5	0.2584	271.8	0.1863	259.5	0.2827	242.8	0.2544
React[13]	271.8	0.0379	263.3	0.0288	269.9	0.1936	253.5	0.076
React[14]	238.2	0.02	236.8	0.0136	265.9	0.0205	241	0.0423
React[15]	236.9	0.017	236	0.0129	234.1	0.0095	239.2	0.0326
React[16]	235.5	0.0189	235	0.0161	233.5	0.0122	237.4	0.0325
React[17]	230	0.0854	230.4	0.0874	228.9	0.106	233.5	0.0642
React[18]	238.3	0.0429	238.4	0.0419	238.3	0.0486	240.7	0.0332
React[19]	235.4	0.0177	235.5	0.0169	235.6	0.0194	232.2	0.0181
React[20]	240.2	0.0209	238.3	0.0201	237.2	0.0232	245.4	0.0208

The relationship and sensitivity between different objectives of the same case are very similar to the revenue best case. Here we will compare different features among these two cases and explain why they are better at their respective objective.

We have found that the key difference between these two cases are the span of the bulk reactive stage. Case 63 has 5 bulk reactive stages while case 317 only has 4.

	Revenue - 63		Revenue - 317		Profit - 63		Profit - 317	
	Conversion	Reflux Ratio	Conversion	Reflux Ratio	Conversion	Reflux Ratio	Conversion	Reflux Ratio
	90.37%	7.5	90.36%	7.61	90.60%	7.56	90.65%	7.73
	Total Feed	Obj	Total Feed	Obj	Total Feed	Obj	Total Feed	Obj
	10	22.328	10	22.313	9.089	2.128	8.878	2.155
	Feed (kmol/s)	Catalyst (kg)	Feed (kmol/s)	Catalyst (kg)	Feed (kmol/s)	Catalyst (kg)	Feed (kmol/s)	Catalyst (kg)
React[13]	0.717	3694	0.013	10	0.472	2830	0.007	10
React[14]	0.937	4538	0.864	4257	0.785	4530	0.755	4590
React[15]	1.066	4627	1.106	4999	0.959	4969	1.024	5658
React[16]	1.006	4435	1.111	4991	1.032	5125	1.125	5826
React[17]	0.001	9849	0.001	10934	0.001	12379	0.001	13207

In the case of revenue optimization, the feed gas amount is fixed, and we already knew that it is larger than the optimum amount. Therefore, case 63, with one more layer of reactive stage, has the advantage of higher conversion. However, in the case of profit optimization, the total feed gas is optimized as well. Under these circumstances, we can see that case 317, with only 4 layers of reactive stages, has an optimum total feed of 8.878, which is lower than 9.089 of case 63.

To summarize, different solution structures defines the strengths of each model. In the above comparison, we see that case 63 is more suitable to handle larger amount of feed, while case 317 is more suitable to handle smaller amount of feed. This hypothesis can be supported by examining two cases' subsequent extension 3-1 and 3-2.

Case: 63 3-1		Case: 317 3-1		Case: 63 3-2		Case: 317 3-2	
Conversion	Reflux Ratio	Conversion	Reflux Ratio	Conversion	Reflux Ratio	Conversion	Reflux Ratio
89.77%	8.33	89.72%	8.88	87.56%	7.60	87.60%	7.60
Total Feed	Obj	Total Feed	Obj	Total Feed	Obj	Total Feed	Obj
8.921	2.773	8.518	2.848	15.770	6.272	15.659	6.241
Feed (kmol/s)	Catalyst (kg)	Feed (kmol/s)	Catalyst (kg)	Feed (kmol/s)	Catalyst (kg)	Feed (kmol/s)	Catalyst (kg)

React[13]	0.013	10	0.006	10	1.287	4026	0.013	10
React[14]	0.529	3258	0.01	10	1.574	4681	1.613	4858
React[15]	0.828	4694	0.668	4138	1.698	4584	1.711	4656
React[16]	1.002	5521	1.096	6692	1.267	4007	1.288	4039
React[17]	0.001	16266	0.001	18943	0.001	5119	0.001	5099

In extension 3-1, we can see although both case 63 and 317 got reduced catalyst bed length due to increased reflux tray location, case 63 still holds one more reactive tray. As a result, its performance dealing with smaller total feed is worse than case 317's. On the contrary, for extension 3-2, we can see that because feed is cheaper, case 63 favors larger feed amount and outperforms case 317.

3.5 Comparison with Reactive Flash

To illustrate the advantage of using reactive flash distillation for FT process, we solved the same profit optimization (3) using a reactive flash model and compare both solutions

3.5.1 Methods

The biggest challenge for a fair comparison between reactive flash and reactive distillation is how to simulate the degree of separation achieved through distillation after a reactive flash, since reactive flash outputs only raw liquid and vapor stream. Obviously, the best way to achieve it is by simulating and optimizing a combined reactive flash and distillation column, which is out of the scope of this work.

In this study, we will emulate the separating effectiveness of a distillation column by imposing an arbitrary relative separation coefficient, which we can extract from the optimum profit case 317. We define the following variable, represents the percentage of a certain components separated into certain outlet streams. ($i = components, p = product\ streams$)

$$\beta_{i,p} = \frac{F_p \cdot xp_{i,p}}{\sum_p (F_p \cdot x_{i,p}) + V_{condenser} \cdot y_i + W_{water} \cdot x_i}$$

We will apply the coefficient matrix to the outlet of reactive flash and compute the total flow of each outlet streams. Recall that the mass balance of reactive distillation column includes all products, vapor outlet and water from condenser. Overall, the product flow of the distillation process following the reactive flash is computed as follows.

$$F_p = \sum_i (L_{RF} \cdot x_i + V_{RF} \cdot y_i) \cdot \beta[i,p]$$

Since the products share the same relative separation coefficient with reactive distillation, it is natural that they have the same selling price in the objective.

Step	C1-C4 & Gas	Naphtha	Heavy Naphtha	Gasoline	Diesel	Heavy	Tray	Feed
Profit	1.3	43	20	90	128	100	N/A	-2.24

3.5.2 Results and Comparison

There are two degrees of freedom in the reactive flash case: temperature and total feed flow. Among the two, temperature is adjusted for optimum selectivity by the weight vector. The feed flow, while technically should be relaxed, is fixed to be the same as reactive distillation case 317. As a result, we can have a direct horizontal comparison on the two cases.

	Reactive Flash	Reactive Distillation
Profit (3)	2.28 (no separation cost)	2.16
Temperature	230.8	230.4 (largest tray)
Feed	8.88	8.88
C1-C4 & Gas	1.901	1.4284
Naphtha	0.0633	0.0679
Gasoline	0.1122	0.1172
Diesel	0.0383	0.0380
Heavy	0.0198	0.0185
r_FT	2.53	2.60
Yield*	85%	88%

* Represents the percentage of carbon converted from feed to FT product, as opposed to competing water-gas-shift reaction.

Note that although reactive flash scores a better economic objective than reactive distillation, it is done by assuming no cost associated with separation. Therefore, the focus here should be the yield and FT reaction extent. We can easily see that reactive distillation offers better yield and FT reaction extent from the table above. By analyzing internal variables such as gas fugacity, we have found that the reason why reactive distillation, not only offers separation, but also more reaction.

Typically, a FT reaction is not an equilibrium constrained reaction. However, its reactants, CO, H_2 and H_2O are subject to water shift reaction, which is an equilibrium reaction. In addition, FT reaction produces a lot of H_2O as by-product during C-chain growth. Therefore, inside a FT reactive flash, the water content will be accumulated and starts to convert CO into

CO_2. Not only that, the increase in water content also reduces the partial pressure of CO and H_2, which in turn directly reduces the rate of reaction.

By plotting the internal fugacity of trays in a reactive distillation and compare it with the internal fugacity of a reactive flash, we found the following:

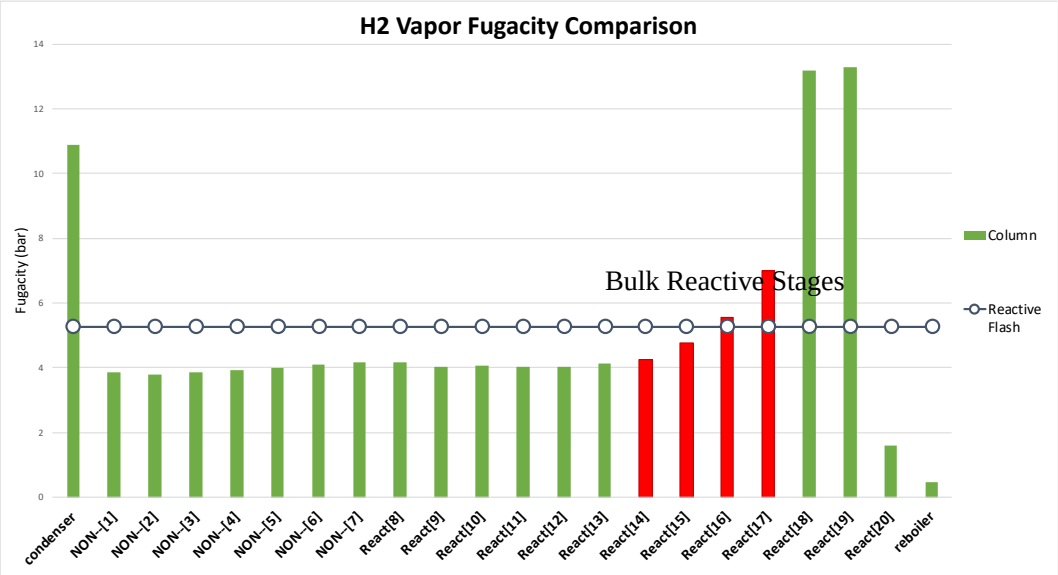

For most parts of the reactive distillation column, the internal fugacity of H_2 is diluted by the constant reflux and vapor flow. However, during certain regions near the bottom where feed comes in, we can see clearly that tray 17 and tray 16 have higher H_2 fugacity. Now if we look at the optimized solution, we will find that the design takes advantage of that and put most of the catalyst inside those trays.

	Feed (kmol/s)	Catalyst (kg)
React[13]	0.007	10
React[14]	0.755	4590
React[15]	1.024	5658
React[16]	1.125	5826
React[17]	0.001	13207

Now if we plot a weighted square of the product between catalyst loading and H_2 fugacity, we can find that the “integration” of reactive distillation outweighs reactive flash.

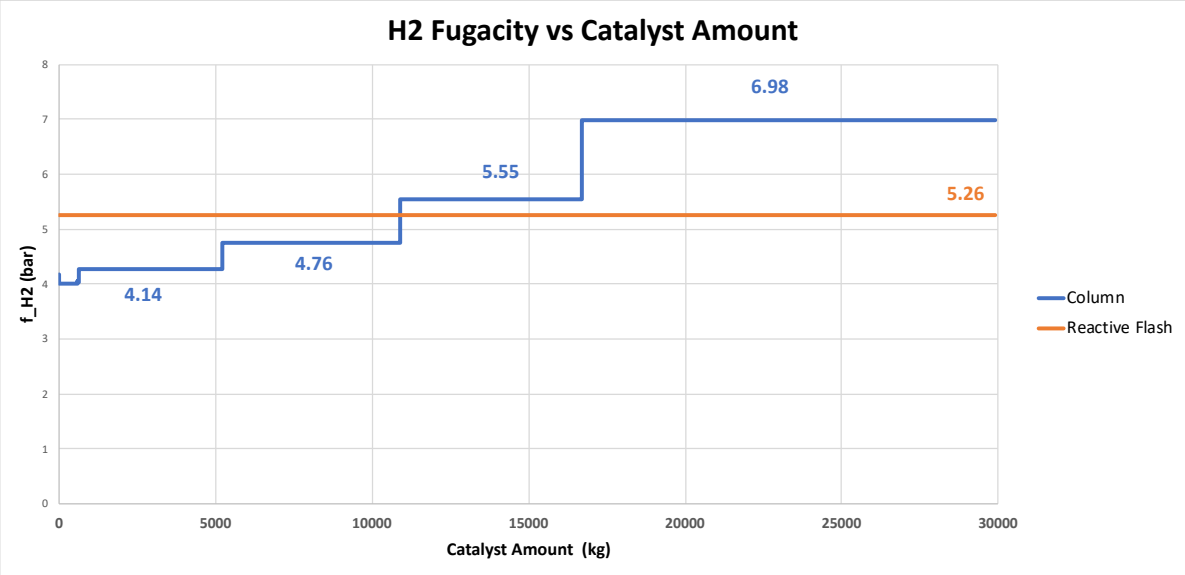

Overall, the comparison shows a 20% increase in overall throughput, and an average of 24% increase in product production, which yields a 45% increase in profit.

	Baseline	Optimum	+%
Total Feed (kmol/s)	7.33	8.88	21.1%
Naphtha (kmol/s)	0.0536	0.0679	26.7%
Gasoline (kmol/s)	0.0963	0.1172	21.7%
Diesel (kmol/s)	0.0307	0.0380	23.8%
Heavy (kmol/s)	0.0151	0.0185	22.5%
Profit	1.47	2.15	46.3%

Recall that in previous discussions, during PCA analysis, we have found that PC2's loading favors high catalyst count in the lower half of the section, which can be explained nicely here.

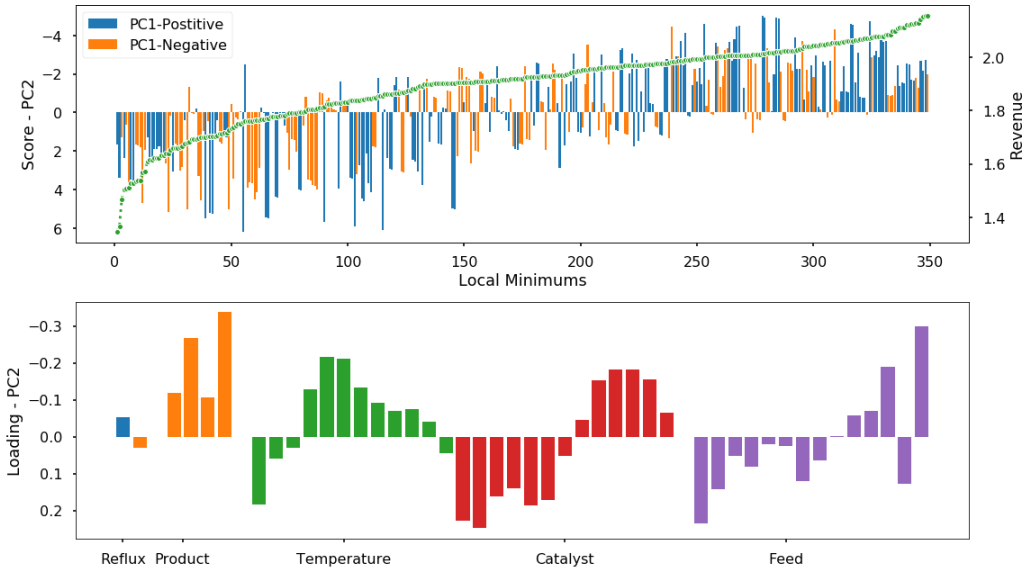

4 Conclusion

In this work, a FT reactive distillation column was modelled using previously developed modelling framework in Pyomo. The model includes kinetic equations, vapor liquid equilibrium equations, energy equations and the MESH equations. Auxiliary formulations, such as mathematical programming with complementary constraints and differentiable distribution function, are used to enhance the model's ability to navigate through phase transitions as well as simultaneously optimize discrete variables.

As demonstrated in previous works, initialization process for reactive distillation, in general, can be very difficult. In this work, a reduced multi-start method is proposed. By removing complicating constraints and assigning variable values as a part of multi-start algorithm, the model become significantly easier to solve and thus can be initialized using a sequential initialization algorithm. After that, the model is considerable closer to the actual feasibility region and can be optimized simultaneous. A 90% initialization success rate and 65% optimization success rate are reported.

The optimization results showed a large number of local minimums with a wide range of objectives, which further supports the necessity of adding a globalization algorithm to the solution strategy. Referencing the best design, we have found that it includes a lot of the features that we would expect from optimizing such distillation column, with the location or values for such features optimized simultaneously. As a result of these optimized design features, we have

found a 45% increase in overall profit, when compared with a base line slurry phase reactor coupled with the same distillation capacity.

Multi-start solutions can be further interpreted by reducing the operability dimension using PCA. As expected, the reduced dimensions can be shown to be collocated with the objective and we have found the best-valued region specific to this problem set-up. We have also showed that the initial values chosen in multi-start algorithm can also be correlated to the final solution, and that a focused initialization in that area could increases the chances of finding better objectives.

5 Bibliography

Bukur, D., Lang, X., & Ding, Y. (1999). Pretreatment effect studies with a precipitated iron Fischer–Tropsch catalyst in a slurry reactor. *Applied Catalysis A: General*, *186*(1-2), 255-275. doi: 10.1016/s0926-860x(99)00148-9

Bukur, D., Nowicki, L., & Lang, X. (1994). Fischer-tropsch synthesis in a stirred tank slurry reactor. *Chemical Engineering Science, 49*(24), 4615-4625. doi: 10.1016/s0009-2509(05)80045-4

Burgard, A., Eason, J., Eslick, J., Ghouse, J., Lee, A., Biegler, L., & Miller, D. (2018). A Smooth, Square Flash Formulation for Equation-Oriented Flowsheet Optimization. In *13th International Symposium on Process Systems Engineering – PSE 2018*. San Diego, California, USA: 2018 Elsevier B.V.

Dry, M. (2002). The Fischer–Tropsch process: 1950–2000. *Catalysis Today*, *71*(3-4), 227-241. doi: 10.1016/s0920-5861(01)00453-9

Groenen, P., & Heiser, W. (1996). The tunneling method for global optimization in multidimensional scaling. *Psychometrika*, *61*(3), 529-550. doi: 10.1007/bf02294553

Heidman, J., Tsonopoulos, C., Brady, C., & Wilson, G. (1985). High-temperature mutual solubilities of hydrocarbons and water. Part II: Ethylbenzene, ethylcyclohexane, and n-octane. *Aiche Journal*, *31*(3), 376-384. doi: 10.1002/aic.690310304

Hogg, J., & Scott, J. (2013). On the effects of scaling on the performance of Ipopt. Retrieved from https://arxiv.org/abs/1301.7283

Marano, J., & Holder, G. (1997). Characterization of Fischer-Tropsch liquids for vapor-liquid equilibria calculations. *Fluid Phase Equilibria, 138*(1-2), 1-21. doi: 10.1016/s0378-3812(97)00166-0

Marano, J., & Holder, G. (1997). General Equation for Correlating the Thermophysical Properties of n-Paraffins, n-Olefins, and Other Homologous Series. 2. Asymptotic Behavior Correlations for PVT Properties. *Industrial & Engineering Chemistry Research, 36*(5), 1895-1907. doi: 10.1021/ie960512f

Masuku, C., Hildebrandt, D., & Glasser, D. (2012). Olefin pseudo-equilibrium in the Fischer–Tropsch reaction. *Chemical Engineering Journal*, *181-182*, 667-676. doi: 10.1016/j.cej.2011.12.052

Masuku, C., Ma, W., Hildebrandt, D., Glasser, D., & Davis, B. (2012). A vapor–liquid equilibrium thermodynamic model for a Fischer–Tropsch reactor. *Fluid Phase Equilibria*, *314*, 38-45. doi: 10.1016/j.fluid.2011.10.020

MOBIL RESEARCH AND DEVELOPMENT CORP. (1982). *SLURRY FISCHER-TROPSCH/MOBIL TWO-STAGE PROCESS OF CONVERTING SYNGAS TO HIGH-OCTANE GASOLINE, QUARTERLY REPORT*. PAULSBORO, NJ.

Srinivas, S., Malik, R., & Mahajani, S. (2008). Feasibility of Reactive Distillation for Fischer−Tropsch Synthesis. *Industrial & Engineering Chemistry Research*, *47*(3), 889-899. doi: 10.1021/ie071094p

U.S. Department of Energy Pittsburgh Energy Technology Center. (1992). *Baseline Design/Economics for Advanced Fischer-Tropsch Technology*.

Zhang, Y., Masuku, C., & Biegler, L. (2018). Equation-Oriented Framework for Optimal Synthesis of Integrated Reactive Distillation Systems for Fischer–Tropsch Processes. *Energy & Fuels*, *32*(6), 7199-7209. doi: 10.1021/acs.energyfuels.8b00971